ELSEVIER

Polymer 41 (2000) 1799–1815

polymer

Evolution of polymer blend morphology during compounding in a twin-screw extruder

Je Kyum Lee, Chang Dae Han*

Department of Polymer Engineering, The University of Akron, Akron, OH 44325-0301, USA

Received 9 January 1999; received in revised form 28 April 1999; accepted 3 May 1999

Abstract

The evolution of blend morphology during compounding in a twin-screw extruder was investigated, putting emphasis on the effects of viscosity ratio, blend composition, and processing variables (barrel temperature profile and screw speed). For the study, we employed the following four blend systems: (i) polystyrene (PS)/poly(methyl methacrylate) (PMMA), (ii) PS/polycarbonate (PC), (iii) PS/high-density polyethylene (HDPE), and (iv) PS/polypropylene (PP). The choice of the above four blend systems was based on the difference in the melting temperature (T_m) of a crystalline polymer and the critical flow temperature (T_{cf}) of an amorphous polymer. Here T_{cf} is defined to be approximately 55°C above the glass transition temperature (T_g) and an amorphous polymer may be considered to *flow* at $T \geq T_{cf}$. The viscosities of the five polymers (PS, PMMA, PC, HDPE, and PP) chosen for melt blending were measured over a wide range of temperatures at shear rates ranging from 0.001 to 1000 s^{-1}. We conducted a 'screw pullout' experiment to investigate the evolution of blend morphology, determined by transmission or scanning electron microscopy, along the extruder axis. We found that the initial blend morphology depends very much on the difference in T_{cf} or T_m between the constituent components and, also, on the viscosities of the constituent components. We observed that a co-continuous morphology was formed at the front end of the extruder, which then transformed into a dispersed morphology towards the end of the extruder. We found that the blend ratio determined the state of dispersion for asymmetric blend compositions and the viscosity ratio determined the state of dispersion for the symmetric blend composition.

Keywords: Polymer blends; Co-continuous morphology; Dispersed morphology

1. Introduction

The morphology of immiscible polymer blends has been a subject of intense research for a long time. There are too many papers to cite them all here. In spite of much efforts spent on the subject since the earlier publications [1–6] in the 1970s, few new scientific revelations have been made during the past two decades. Among various types of mixing equipment, twin-screw extruders have most widely been used to prepare polymer blends in industry. Consequently, during the past decade numerous research groups have investigated morphology development of polymer blends in a twin-screw extruder. There are too many papers to cite them all here and the readers are referred to some recent papers [7–14]. In spite of much effort spent, we still do not have a clear understanding of the morphology evolution in immiscible polymer blends, during compounding in a twin-screw extruder, as affected by the rheological properties of the constituent components, blend composition, and processing variables.

Let us consider the situation where two crystalline polymers, A and B, are compounded in a twin-screw extruder, as shown schematically in Fig. 1, and assume that the melting point ($T_{m,A}$) of polymer A is lower than the melting point ($T_{m,B}$) of polymer B. Thus, at the front end of the extruder where polymer A melts first, the mixture is a suspension consisting of molten polymer A that forms the continuous phase and solid polymer B. As the suspension moves along the extruder axis and reaches a temperature at which polymer B starts to melt, a liquid mixture will form a dispersed morphology, where droplets of polymer B are dispersed in the matrix of polymer A. There are two possibilities: either the same mode of dispersion persists along the rest of the extruder or a phase (or matrix) inversion may take place, where polymer B now becomes the continuous phase and polymer A becomes the discrete phase. That is, a transformation from one mode of dispersion (where polymer B is dispersed in polymer A) to another mode of dispersion (where polymer A is dispersed in polymer B) may take place. What is of great importance is the determination of

* Corresponding author. Tel.: +1-330-972-6468; fax: +1-330-972-5720.
E-mail address: edhan@uakron.edu (C.D. Han)

0032-3861/00/$ - see front matter
PII: S0032-3861(99)00325-0

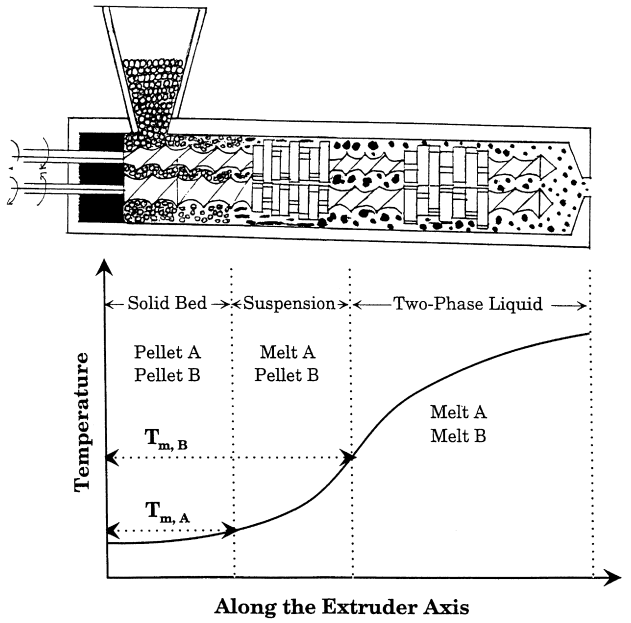

Fig. 1. Schematic diagram describing a twin-screw extruder, in which a pair of immiscible polymers are extruded under a preset temperature profile along the extruder axis.

the conditions under which phase inversion may take place. In our previous study [15] where an internal mixer was employed to investigate the morphology evolution in immiscible polymer blends, we have shown that a co-continuous morphology can be made to transform into a dispersed morphology by either increasing the rotor speed of the mixer and/or melt blending temperature, and a co-continuous morphology is a transitory morphological state, through which one mode of a dispersed morphology transforms into another mode.

In this study, using a twin-screw extruder we investigated the morphology evolution in immiscible polymer blends. Morphology of a polymer blend was identified using scanning electron microscopy (SEM) or transmission electron microscopy (TEM). For the study we chose four pairs of polymers on the basis of (i) the difference in the critical flow temperature (T_{cf}) of two amorphous polymers or (ii) the difference between the melting point (T_m) of a crystalline polymer and the T_{cf} of an amorphous polymer. Earlier, Han et al., [16] defined T_{cf} to be approximately 55°C above the glass transition temperature (T_g) of an amorphous polymer, which was based on the numerical simulations of the extrusion characteristics of an amorphous polymer (polystyrene; polycarbonate) in a single-screw extruder and a comparison of measured pressure profiles along the extruder axis with model prediction. According to Han et al. [16], T_{cf} is a critical temperature at which an amorphous polymer may be regarded as 'liquid' from a rheological point of view and thus an amorphous polymer may be considered to *flow* at $T \geq T_{cf}$. Thus the T_{cf} of an amorphous polymer is de facto equivalent to the 'melting point' of a crystalline polymer. The interested readers are referred to the original paper [16].

The primary objectives of the present study were (1) to interpret the experimentally observed morphology evolution in immiscible polymer blends with the aid of the difference in T_m or T_{cf} of the constituent components, (2) to determine the processing conditions under which a co-continuous morphology may be formed, and (3) to investigate whether or not a co-continuous morphology, if formed, is stable. Emphasis was placed on identifying the factors that determine morphology development in each of the four blend systems investigated. In this paper we report the highlights of our findings.

2. Experimental

2.1. Materials

We employed five commercial polymers: polystyrene (PS), poly(methyl methacrylate) (PMMA), polycarbonate (PC), high-density polyethylene (HDPE), and polypropylene (PP), as summarized in Table 1. Also given in Table 1 are the T_ms of HDPE and PP, and the T_gs of PS, PMMA, and PC. The values of T_m and T_g were determined using differential scanning calorimetry during heating at a rate of 20°C/min. Using these homopolymers we investigated the morphology evolution, during melt blending in a twin-screw extruder, in each of the following four binary blend systems: (i) PMMA/PS, (ii) PC/PS, (iii) PS/HDPE, and (iv) PS/PP, as summarized in Table 2. Also given in Table 2 are (i) the values of ΔT_{cf} between two amorphous polymers, PMMA/PS and PC/PS blends, and (ii) the values of $|T_{cf} - T_m|$ between an amorphous polymer and a crystalline polymer, PS/HDPE and PS/PP blends. As will be shown later in this paper, the concept of T_{cf} is very important to interpret the morphology evolution in PMMA/PS, PC/PS, PS/HDPE, and PS/PP blends during melt blending in a twin-screw extruder.

2.2. Mixing equipment and experimental procedures

Melt blending of a pair of polymers was conducted using a 30 mm co-rotating twin-screw extruder (Japan Steel Works Labotex 30). The screw configuration employed

Table 1
Molecular characteristics of polymers studied

Sample code	Manufacturer	Morphology	T_g or T_m (°C)
PMMA	Rohm and Haas (Plexiglas V825)	Amorphous	118
PS	Dow Chemical (STYRON 615PR)	Amorphous	98
PC	Dow Chemical	Amorphous	146
PP	Exxon Chemical (Escorene 1052)	Crystalline	165
HDPE	Dow Chemical (HF-1030 INSITE)	Crystalline	125

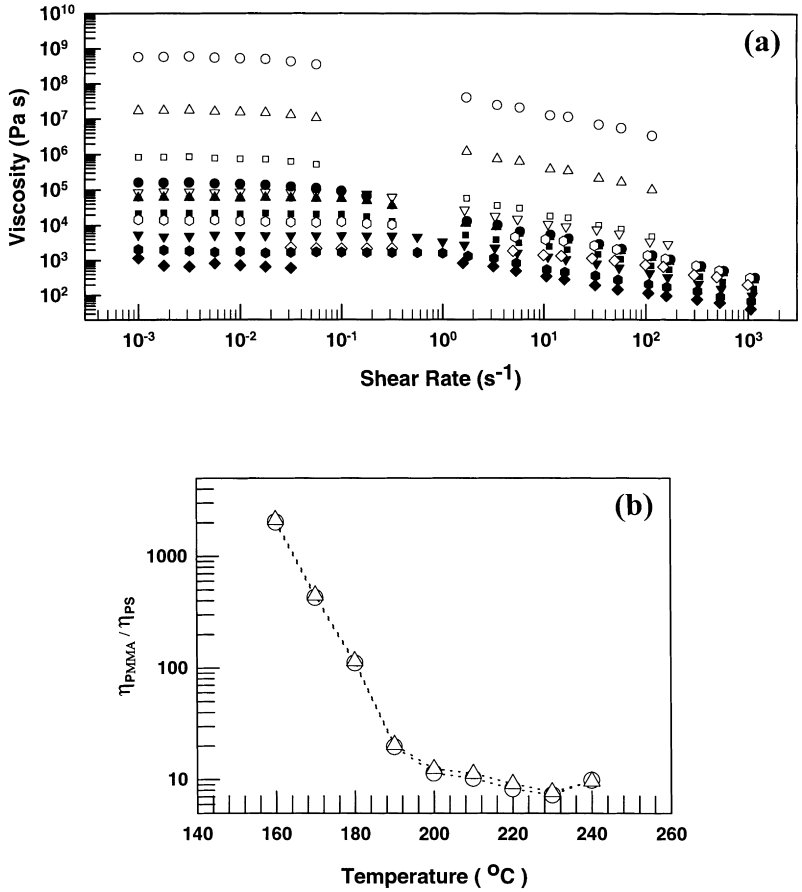

Fig. 2. The upper panel describes the shear rate dependence of viscosity for PMMA (open symbols) and PS (filled symbols) at various temperatures: (○, ●) 160°C; (△, ▲) 170°C; (□, ■) 180°C; (▽, ▼) 200°C; (○, ●) 220°C; (◇, ◆) 240°C. The lower panel describes the temperature dependence of viscosity ratio, η_{PMMA}/η_{PS}, at $\dot{\gamma} = 1500\ s^{-1}$ (○) and at $\dot{\gamma} = 412\ s^{-1}$ (△).

had three kneading blocks. The screw speed of 200 rpm was used for every blend pair except for the 70/30 PC/PC blend (100 rpm), and the throughput of 12 kg/h. At the end of the extruder a 2-hole strand die was attached. In our experiment, two polymers at a given blend ratio were tumbled in a drum for about 30 min before being fed into the hopper of the extruder. Before beginning the extrusion experiment, the barrel temperature was set in accordance with a predetermined temperature profile along the extruder axis. Needless to say, the temperature profiles employed were different for the different polymer pairs extruded. At the end of each extrusion run, the screw was quenched rapidly to minimize variations of blend morphology and pulled out. The specific temperature profiles employed will be shown below when presenting the micrographs of blend specimens for each polymer pair, describing morphology evolution along the extruder axis. The positions at which blend specimens were taken after screw pullout will also be indicated on each micrograph.

2.3. Microscopy

A blend specimen was first embedded in an epoxy (EPON 828) and cured at room temperature using 10 wt% triethylenetetramine; complete curing took about 24 h. The embedded samples were then ultramicrotomed using a Reichert Ultracut S (Leica) microtome equipped with glass knives. In order to have sufficient phase contrast in a melt-blended sample before using a microscope, the following methods were used, namely, PS was etched out selectively using toluene from PC/PS, PS/HDPE and PS/PP blend samples. A carbon black coating was applied to the PMMA/PS blend samples after ultramicrotoming. A transmission electron microscope (JEM 1200EX II, JEOL) operated at 120 kV was used to take micrographs of the PMMA/PS blend specimens. A scanning electron microscope (Hitachi, Model S-2150) was used to observe the phase morphology of PC/PS, PS/HDPE, and PS/PP blend specimens.

2.4. Rheological measurement

A Rheometrics mechanical spectrometer (Model RMS 800) with cone-and-plate fixture (25 mm diameter and 5° cone angle) was used, under a nitrogen atmosphere, to measure the shear viscosities of the five homopolymers

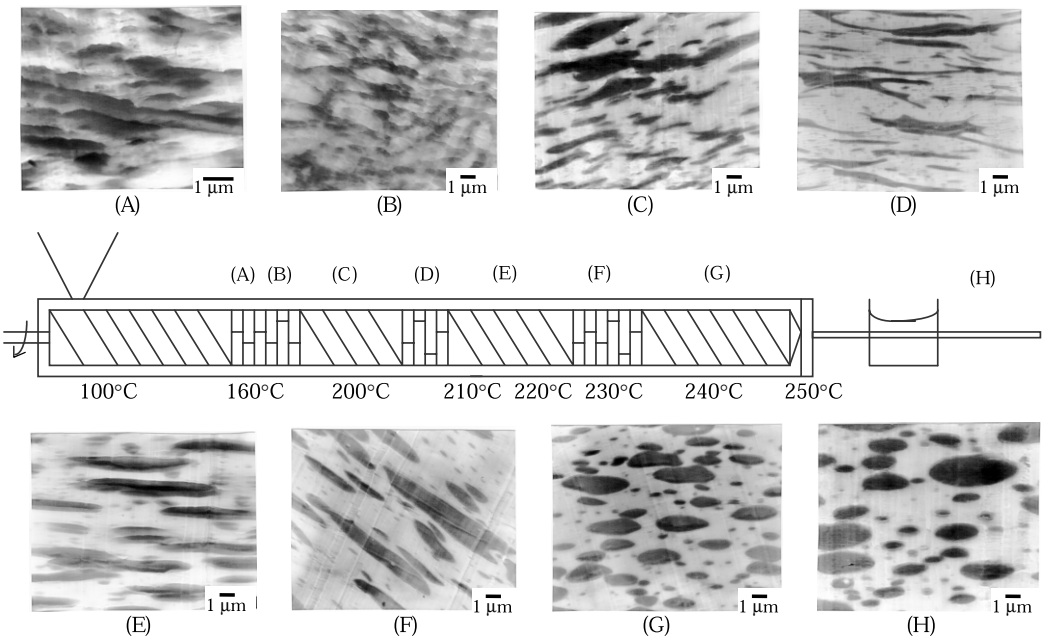

Fig. 3. The evolution of morphology in 70/30 PMMA/PS blend during compounding in a twin-screw extruder: (A) at the front end of the first kneading block (160°C); (B) at the exit of the first kneading block (160°C); (C) between the first and second kneading blocks (200°C); (D) at the front end of the second kneading block (200°C); (E) between the second and third kneading blocks (220°C); (F) at the exit of the third kneading block (230°C); (G) between the third kneading block and the die (240°C); (H) extrudate.

(PS, PMMA, PC, HDPE, and PP) over a very wide range of temperatures at low shear rates ranging from 0.001 to ca. 10 s^{-1}. An Instron capillary rheometer (Mode 3211, Instron Corporation) with a capillary diameter of 0.15 cm and a length-to-diameter ratio of 28.5 was used to measure the viscosities of the same homopolymers at high shear rates ranging from ca. 10 to 1000 s^{-1}.

3. Results

3.1. Morphology evolution in blends consisting of two amorphous polymers

3.1.1. PMMA/PS blends

Fig. 2(a) describes the dependence of viscosity of PMMA and PS, respectively, on shear rate ($\dot{\gamma}$) at various temperatures ranging from 160 to 240°C, and Fig. 2(b) describes the dependence of viscosity ratio, η_{PMMA}/η_{PS}, on temperature at $\dot{\gamma} = 1500\ s^{-1}$ and $\dot{\gamma} = 412\ s^{-1}$, respectively. It can be seen in Fig. 2 that the viscosity of PMMA is much higher than that of PS over the entire range of temperatures and shear rates tested.

Fig. 3 gives TEM images describing the morphology evolution in 70/30 PMMA/PS blend along the extruder axis, and a schematic describing barrel temperature profile and positions where blend specimens were taken after 'screw pullout'. In Fig. 3 the dark areas represent PS and the light areas represent PMMA. The following observations are worth noting on the morphology evolution displayed in Fig. 3. At the front end of the first kneading block (position A) we observe a co-continuous morphology. Although the barrel temperature at position A was set at 160°C, we are quite certain that owing to viscous shear heating, the real temperature of the blend must have been higher than 160°C. In view of the fact that the T_{cf} of PS is 155°C and that of PMMA is 170°C (see Table 2), it is reasonable to speculate that the PMMA in the 70/30 PMMA/PS blend barely began to flow at position A. At the exit of the first kneading block (position B) we observe some breakdown of interconnected structures of PMMA that are dispersed in the PS phase. At position C, where the barrel temperature was set at 200°C, we clearly observe a dispersed morphology in which elongated droplets of PS are dispersed in the PMMA matrix. It is interesting to note that the PMMA phase broken down at position B apparently underwent coalescence, forming a continuous phase at position C, i.e. a phase inversion took place inside the extruder.

Table 2
Polymer pairs employed for preparing blends

Sample code	Morphology	ΔT_{cf}, $\lvert T_{cf} - T_m \rvert$, or ΔT_m (°C)
PMMA/PS	Amorphous/amorphous	15[a,b]
PC/PS	Amorphous/amorphous	45[c]
PS/HDPE	Amorphous/crystalline	30[a]
PS/PP	Amorphous/crystalline	10[a]

[a] T_{cf} of PS ≈ 155°C.
[b] T_{cf} of PMMA ≈ 170°C.
[c] T_{cf} of PC ≈ 200°C.

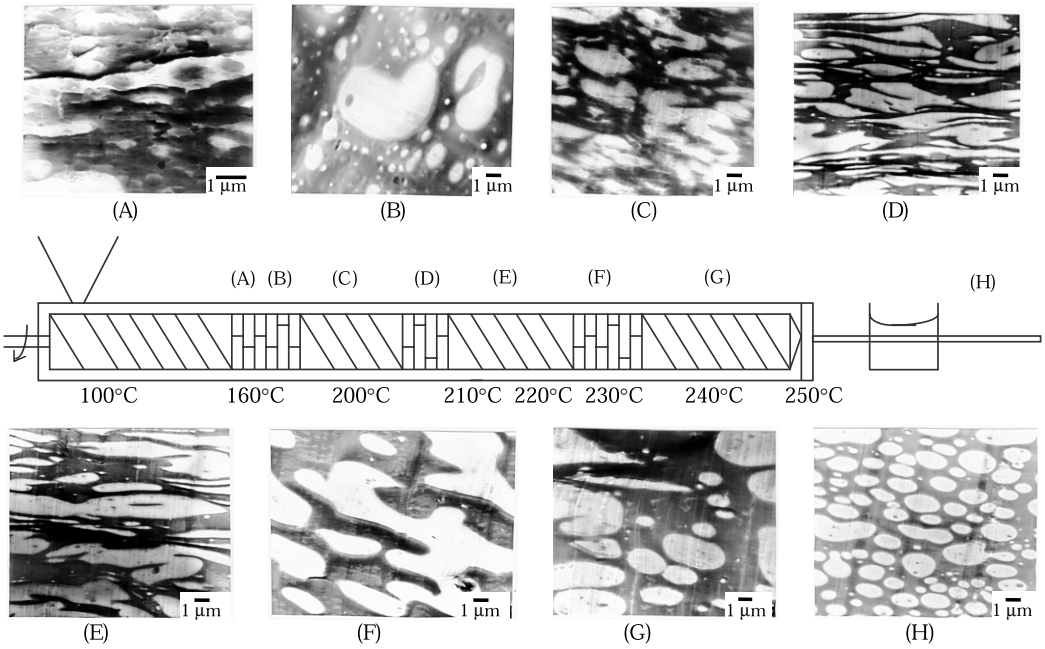

Fig. 4. The evolution of morphology in 50/50 PMMA/PS blend during compounding in a twin-screw extruder: (A) at the front end of the first kneading block (160°C); (B) at the exit of the first kneading block (160°C); (C) between the first and second kneading blocks (200°C); (D) at the front end of the second kneading block (200°C); (E) between the second and third kneading blocks (220°C); (F) at the exit of the third kneading block (230°C); (G) between the third kneading block and the die (240°C); (H) extrudate.

This might have resulted from a slow down of melt flow at position C which consists of screw elements forming mixing chambers, while mixing was very intense at the first kneading block preceding position C. At the second kneading block (position D) we observe a fibrillation of the dispersed PS phase, giving rise to very long threadlike droplets. At position E where the barrel temperature was set at 210–220°C we observe, once again, evidence of droplet coalescence which, as pointed out above, might have resulted from a slow down of melt flow in the mixing chamber past the second kneading block. At position G past the third kneading block we observe both breakup and coalescence of PS droplets. We believe that breakup of droplets at position G (with the barrel temperature set at 240°C) was much easier than at position E (with the barrel temperature set at 210°C), because the viscosities of both PS and PMMA decreased with increasing temperature and the viscosity ratio, η_{PMMA}/η_{PS}, was higher than 10 at temperatures between 160 and 210°C at $\dot{\gamma} = 412\ s^{-1}$ (see Fig. 2), which was estimated to be the average shear rate inside the screw channel. According to the literature [17–20], droplet breakup becomes easier when the viscosity ratio of droplet to medium lies between 0.1 and 1.

When two immiscible liquids are mixed we expect, according to the minimum energy dissipation principle, that the more viscous component will form the discrete phase and the less viscous component will form the continuous phase. Thus, it is reasonable to expect that in 70/30 PMMA/PS mixture the PMMA forms the discrete phase and the PS forms the continuous phase. However, from Fig. 3 we observe that the major component PMMA, though more viscous, forms the continuous phase (matrix) and the minor component PS forms the discrete phase (droplets), contrary to the expectation from the minimum energy dissipation principle. Thus we conclude that in the 70/30 PMMA/PS blend, the blend ratio played a predominant role over the viscosity ratio in determining the state of dispersion.

Fig. 4 gives TEM images describing the morphology evolution in 50/50 PMMA/PS blend along the extruder axis, and a schematic describing barrel temperature profile and positions where blend specimens were taken after 'screw pullout'. The following observations are worth noting on the morphology evolution displayed in Fig. 4. At the front end of the first kneading block (position A), where the barrel temperature was set at 160°C, we observe a mixture of small droplets and very large domains suspended in the PS matrix. Note that at 160°C (though the real melt temperature should have been higher) that is slightly lower than the T_{cf} of PMMA, the mobility of the PMMA in the 50/50 PMMA/PS blend would have been extremely low. Note in Fig. 2 that at 160°C the viscosity of the PMMA is about 2000 times that of the PS. Therefore, adequate mixing between the PMMA and PS in the 50/50 PMMA/PS blend at 160°C would have been very difficult. At the exit of the first kneading block (position B) we observe a breakdown of large PMMA domains, though still present, that are dispersed in the PS phase. At position C where the barrel temperature was set at 200°C we observe coalescence of PMMA droplets, the mechanism for which was presented

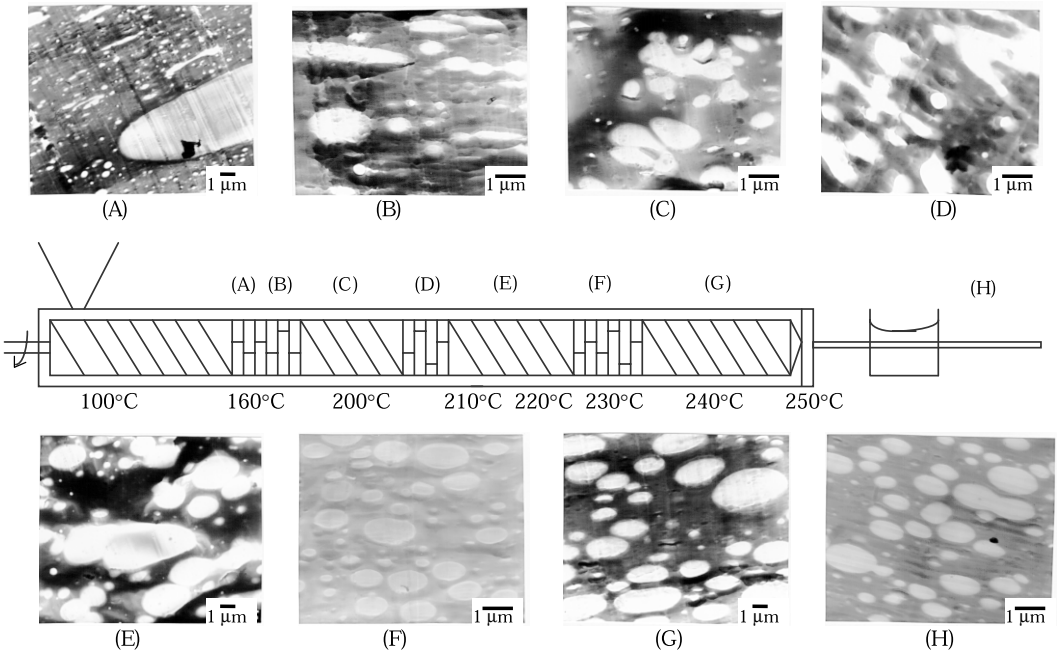

Fig. 5. The evolution of morphology in 30/70 PMMA/PS blend during compounding in a twin-screw extruder: (A) at the front end of the first kneading block (160°C); (B) at the exit of the first kneading block (160°C); (C) between the first and second kneading blocks (200°C); (D) at the front end of the second kneading block (200°C); (E) between the second and third kneading blocks (220°C); (F) at exit of the third kneading block (230°C); (G) between the third kneading block and the die (240°C); (H) extrudate.

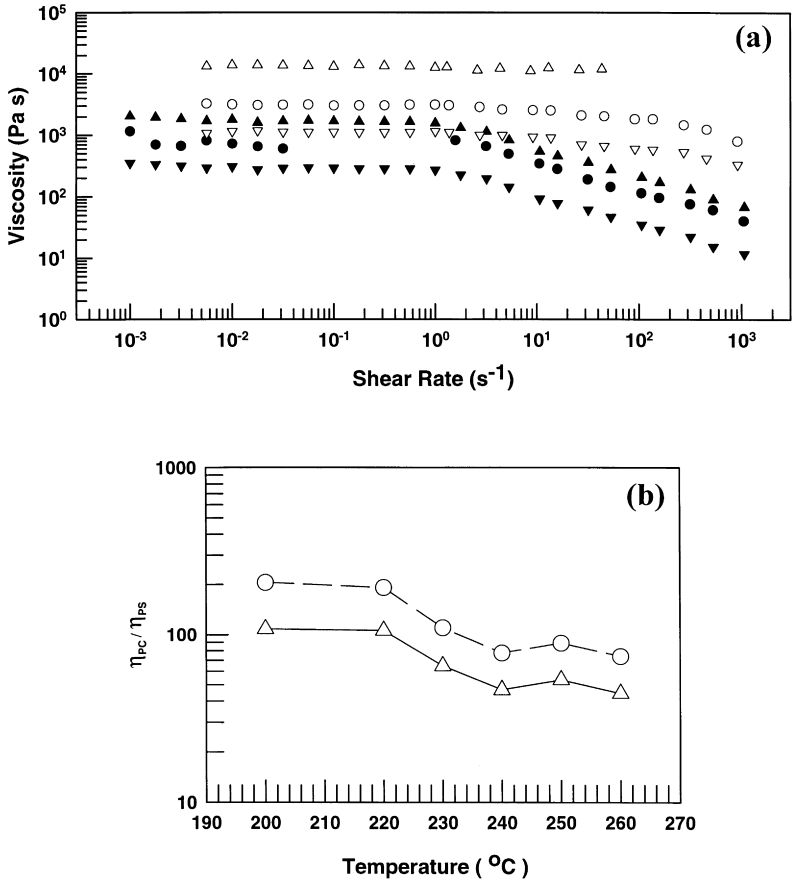

Fig. 6. The upper panel describes the shear rate dependence of viscosity for PC (open symbols) and PS (filled symbols) at various temperatures: (○, ●) 220°C; (△, ▲) 240°C; (▽, ▼) 260°C. The lower panel describes the temperature dependence of viscosity ratio, η_{PC}/η_{PS}, at $\dot{\gamma} = 1500\ s^{-1}$ (○) and at $\dot{\gamma} = 410\ s^{-1}$ (△).

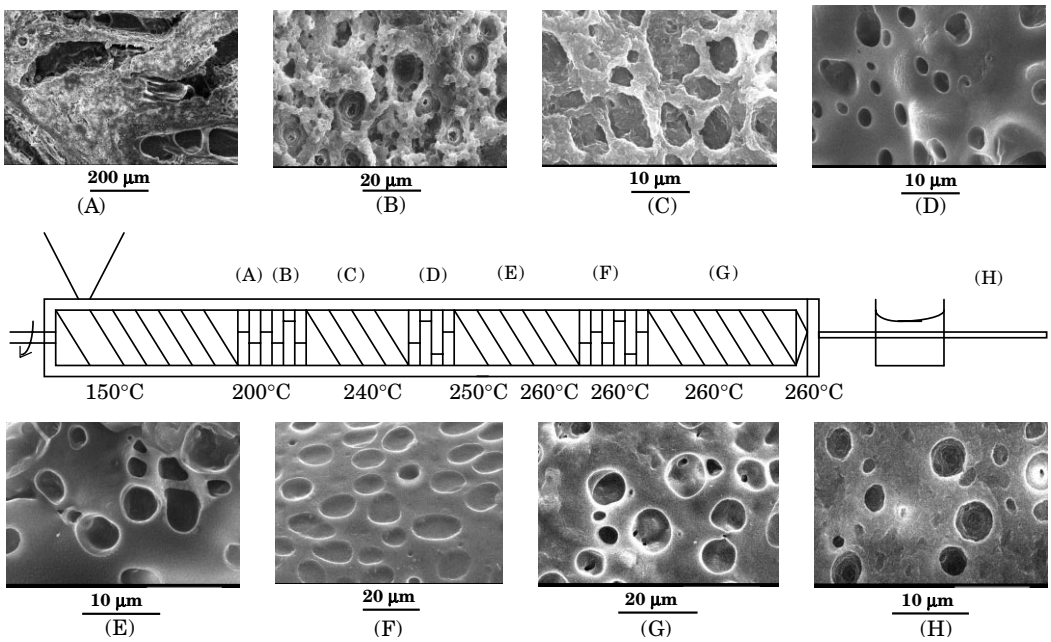

Fig. 7. The evolution of morphology in 70/30 PC/PS blend during compounding in a twin-screw extruder: (A) at the front end of the first kneading block (200°C); (B) at the exit of the first kneading block (200°C); (C) between the first and second kneading blocks (240°C); (D) at the front end of the second kneading block (250°C); (E) between the second and third kneading blocks (260°C); (F) at the exit of the third kneading block (260°C); (G) between the third kneading block and the die (260°C); (H) extrudate.

above. In the second kneading block (position D) we observe an elongation of PMMA droplets, and at position E where the barrel temperature was set at 210–220°C we observe evidence of droplet coalescence. At position G where the barrel temperature was set at 240°C we observe a dispersed morphology, which becomes much more clear in the extrudate (position H). In the 50/50 PMMA/PS blend we observe that the more viscous PMMA forms the discrete phase and the less viscous PS forms the continuous phase. Thus we conclude that in this blend composition, the viscosity ratio played a predominant role over the blend ratio in determining the state of dispersion.

Fig. 5 gives TEM images describing the morphology evolution in 30/70 PMMA/PS blend along the extruder axis, and a schematic describing barrel temperature profile and positions where blend specimens were taken after 'screw pullout'. The following observations are worth noting on the morphology evolution displayed in Fig. 5. At the front end of the first kneading block (position A) we observe a mixture of small droplets and very large domains suspended in the PS matrix. Being the minor component in the 30/70 PMMA/PS blend, the PMMA might have been easier, compared to the other blend compositions considered above, to form the discrete phase in the environment of the less viscous PS phase forming the continuous phase. At the exit of the first kneading block (position B) we observe a breakdown of large PMMA domains as well as coalescence of very small PMMA droplets dispersed in the PS matrix. Along the remainder of the extruder axis, we observe a dispersed morphology in which PMMA droplets are dispersed in the PS matrix. This observation is consistent with the expectation from the minimum energy dissipation principle, stating that the less viscous component would form a continuous phase and the more viscous component would form a discrete phase. After all, the PMMA is the minor component in the 30/70 PMMA/PS blend.

3.1.2. PC/PS blends

Fig. 6(a) describes the dependence of viscosity of PC and PS, respectively, on shear rate ($\dot{\gamma}$) at various temperatures ranging from 220 to 260°C, and Fig. 6(b) describes the dependence of viscosity ratio, η_{PC}/η_{PS}, on temperature at $\dot{\gamma} = 1500\ s^{-1}$ and $\dot{\gamma} = 410\ s^{-1}$, respectively. It can be seen in Fig. 6 that the viscosity of PC is much higher than that of PS over the entire range of temperatures and shear rates tested.

Fig. 7 gives SEM images describing the morphology evolution in 70/30 PC/PS blend along the extruder axis, and a schematic describing barrel temperature profile and positions where blend specimens were taken after 'screw pullout'. The following observations are worth noting on the morphology evolution displayed in Fig. 7. At the first kneading block (positions A and B), where the barrel temperature was set at 200°C, the morphology of the mixture is not well developed. Again, although the barrel temperature was set at 200°C, we are certain that the real temperature of the blend must have been, owing to viscous shear heating, higher than 200°C. It should be remembered that the T_{cf} of PC is about 200°C while the T_{cf} of PS is about 155°C (see Table 2). Therefore, the very viscous PC at 200°C must have prevented a uniform mixing with PS at

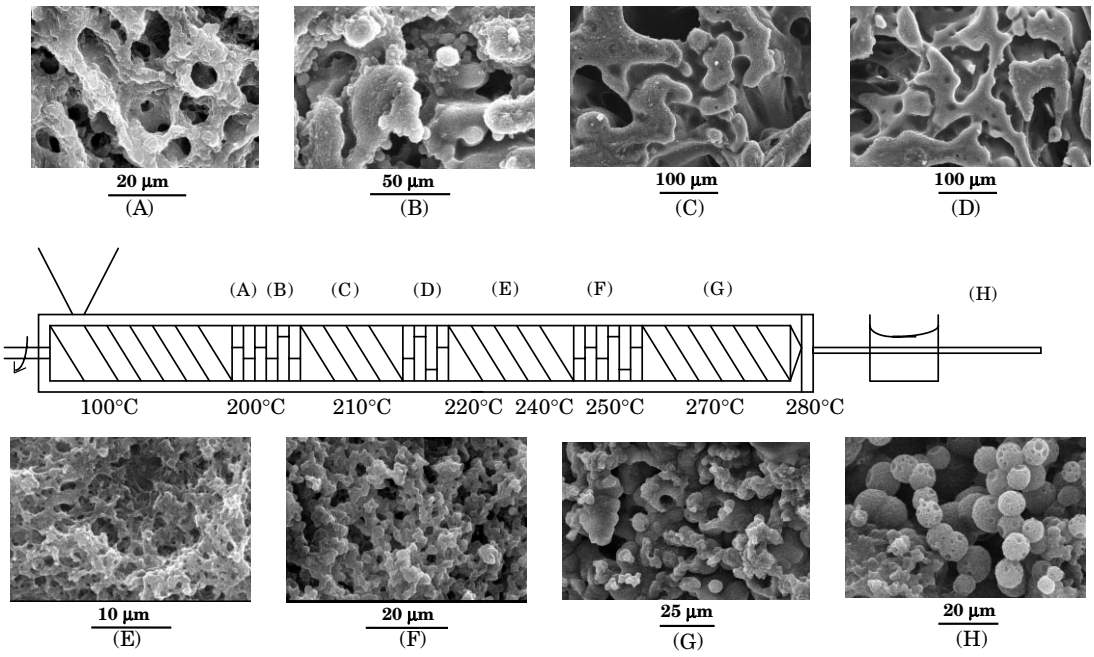

Fig. 8. The evolution of morphology in 50/50 PC/PS blend during compounding in a twin-screw extruder: (A) at the front end of the first kneading block (200°C); (B) at the exit of the first kneading block (200°C); (C) between the first and second kneading blocks (210°C); (D) at the front end of the second kneading block (220°C); (E) between the second and third kneading blocks (240°C); (F) at the exit of the third kneading block (250°C); (G) between the third kneading block and the die (270°C); (H) extrudate.

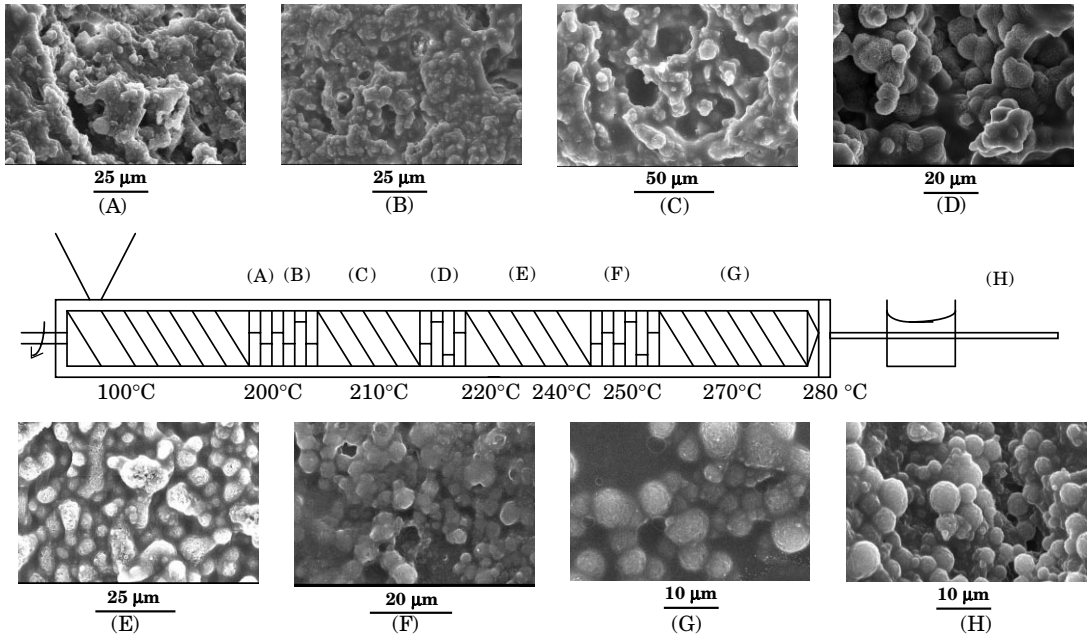

Fig. 9. The evolution of morphology in 30/70 PC/PS blend during compounding in a twin-screw extruder: (A) at the front end of the first kneading block (200°C); (B) at the exit of the first kneading block (200°C); (C) between the first and second kneading blocks (210°C); (D) at the front end of the second kneading block (220°C); (E) between the second and third kneading blocks (240°C); (F) at the exit of the third kneading block (250°C); (G) between the third kneading block and the die (270°C); (H) extrudate.

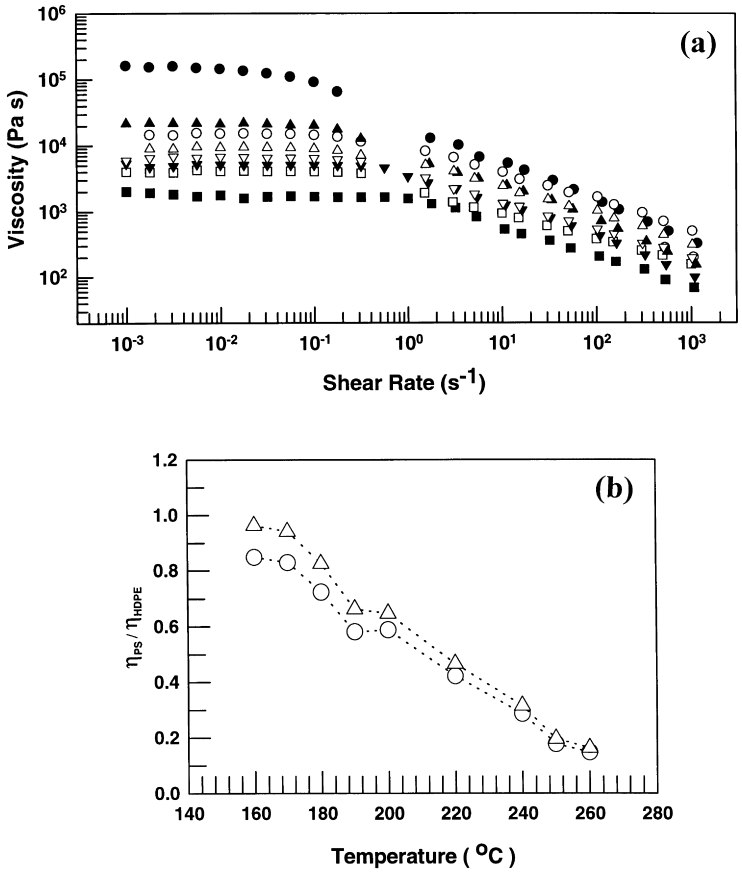

Fig. 10. The upper panel describes the shear rate dependence of viscosity for HDPE (open symbols) and PS (filled symbols) at various temperatures: (○, ●) 160°C; (△, ▲) 180°C; (▽, ▼) 200°C; (□, ■) 220°C. The lower panel describes the temperature dependence of viscosity ratio, η_{PS}/η_{HDPE}, at $\dot{\gamma} = 1500\ s^{-1}$ (○) and at $\dot{\gamma} = 507\ s^{-1}$ (△).

positions A and B. At position C where the barrel temperature was set at 240°C we observe a somewhat improved state of dispersion, and at the second kneading block (position D) and at position E where the barrel temperature was set at 250–260°C, we observe a dispersed morphology in which PS droplets are dispersed in the matrix of PC. Along the remainder of the extruder axis, we observe that the PS forms a discrete phase dispersed in the PC matrix. From Fig. 7 we observe that the major component PC, though more viscous, forms a continuous phase and the less viscous, minor component PS forms a discrete phase. Thus we conclude that blend ratio played a predominant role over the viscosity ratio in determining the state of dispersion in the 70/30 PC/PS blend. This observation is consistent with that made for the 70/30 PMMA/PS blend considered above.

Fig. 8 gives SEM images describing the morphology evolution in 50/50 PC/PS blend along the extruder axis, and a schematic describing barrel temperature profile and positions where blend specimens were taken after 'screw pullout'. The following observations are worth noting on the morphology evolution displayed in Fig. 8. At the first kneading block (positions A and B) we observe a morphology in which highly interconnected structures of PC are suspended in the PS matrix. At position C where the barrel temperature was set at 210°C the state of morphology improved little, while in the second kneading block (position D) we observe some breakdown of the interconnected structures of PC. At position E where the barrel temperature was set at 220–240°C we observe many small domains of PC that resulted from a breakdown of all the interconnected structures of PC, and at position G where the barrel temperature was set at 270°C we observe a dispersed morphology in which PC droplets, still agglomerated somewhat, are dispersed in the PS matrix. We observe a well-developed dispersed morphology in the extrudate (position H). From this observation we conclude that the viscosity ratio played a predominant role over the blend ratio in determining the state of dispersion in the 50/50 PC/PS blend.

Fig. 9 gives SEM images describing the morphology evolution in 30/70 PC/PS blend along the extruder axis, and a schematic describing barrel temperature profile and positions where blend specimens were taken after 'screw pullout'. The following observations are worth noting on the morphology evolution displayed in Fig. 9. At the first kneading block (position A) where the barrel temperature was set at 200°C we observe a very poorly mixed morphology in which highly interconnected structures of PC are suspended in the PS matrix. In the second kneading block

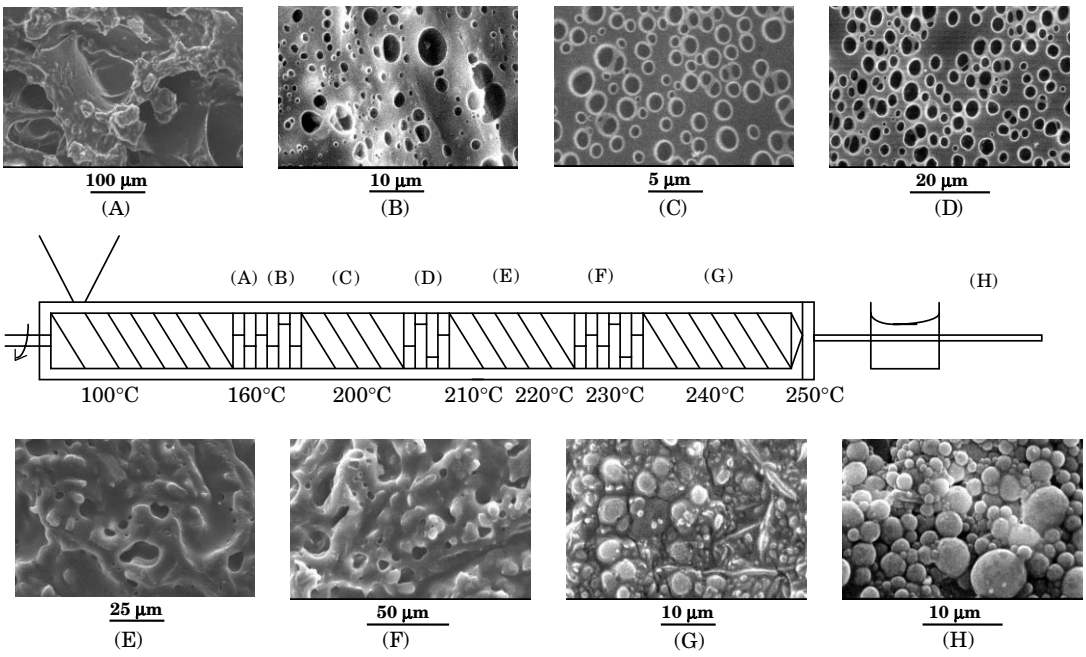

Fig. 11. The evolution of morphology in 70/30 PS/HDPE blend during compounding in a twin-screw extruder: (A) at the front end of the first kneading block (160°C); (B) at the exit of the first kneading block (160°C); (C) between the first and second kneading blocks (200°C); (D) at the front end of the second kneading block (210°C); (E) between the second and third kneading blocks (220°C); (F) at the exit of the third kneading block (230°C); (G) between the third kneading block and the die (240°C); (H) extrudate.

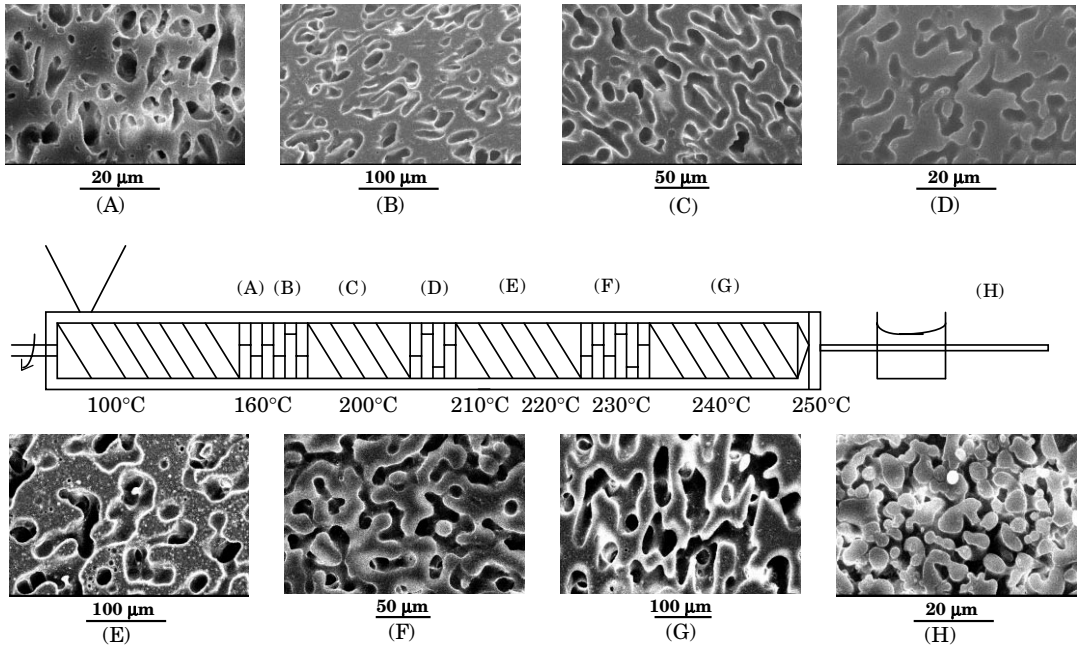

Fig. 12. The evolution of morphology in 50/50 PS/HDPE blend during compounding in a twin-screw extruder: (A) at the front end of the first kneading block (160°C); (B) at the exit of the first kneading block (160°C); (C) between the first and second kneading blocks (200°C); (D) at the front end of the second kneading block (210°C); (E) between the second and third kneading blocks (220°C); (F) at the exit of the third kneading block (230°C); (G) between the third kneading block and the die (240°C); (H) extrudate.

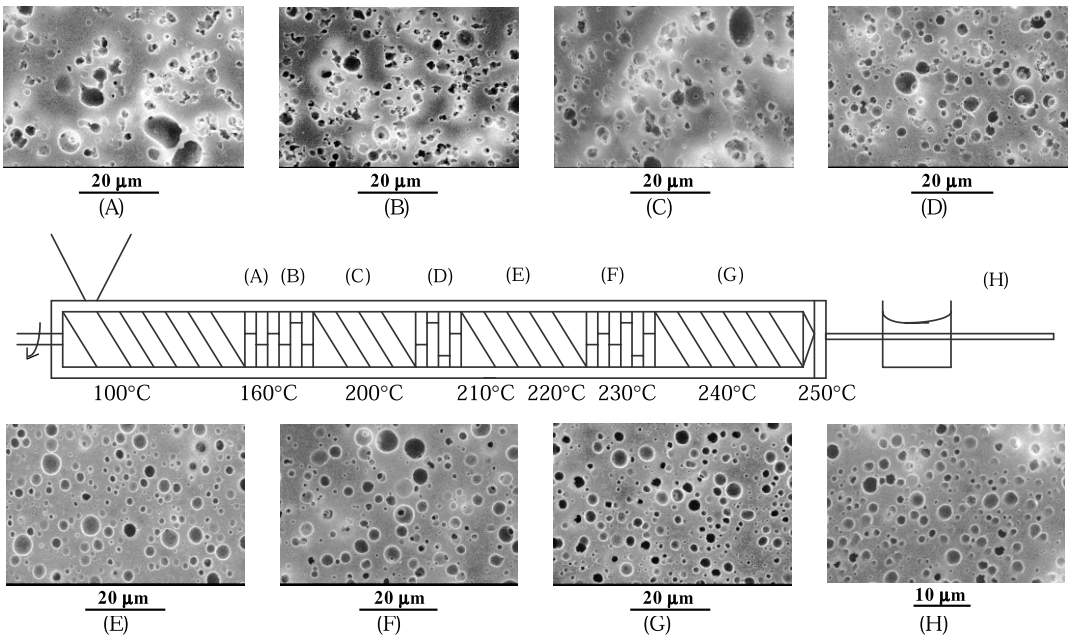

Fig. 13. The evolution of morphology in 30/70 PS/HDPE blend during compounding in a twin-screw extruder: (A) at the front end of the first kneading block (160°C); (B) at the exit of the first kneading block (160°C); (C) between the first and second kneading blocks (200°C); (D) at the front end of the second kneading block (210°C); (E) between the second and third kneading blocks (220°C); (F) at the exit of the third kneading block (230°C); (G) between the third kneading block and the die (240°C); (H) extrudate.

(position D) we observe some breakdown of the interconnected structures of PC and at position E where the barrel temperature was set at 220–240°C we observe a complete breakdown of the interconnected structures of PC. Along the remainder of the extruder axis we observe a dispersed morphology in which the more viscous, minor component PC forms droplets dispersed in the less viscous, major component PS. This observation is consistent with that made above for the 30/70 PMMA/PS blend.

3.2. Morphology evolution in blends consisting of amorphous and crystalline polymers

3.2.1. PS/HDPE blends

Fig. 10(a) describes the dependence of viscosity of PS and HDPE, respectively, on shear rate ($\dot{\gamma}$) at various temperatures ranging from 160 to 220°C, and Fig. 10(b) describes the dependence of viscosity ratio, η_{PS}/η_{HDPE}, on temperature at $\dot{\gamma} = 1500$ and 507 s^{-1}, respectively, showing that η_{PS}/η_{HDPE} decreases with increasing temperature. It can be seen in Fig. 10 that (i) at 160 and 180°C the viscosity of PS is higher than that of HDPE at *low* shear rates, but the viscosities of the two polymers cross each other at higher shear rates, and (ii) at higher temperatures (180–220°C) the viscosity of HDPE becomes higher than that of PS.

Fig. 11 gives SEM images describing the morphology evolution in 70/30 PS/HDPE blend along the extruder axis, and a schematic describing barrel temperature profile and positions where blend specimens were taken after 'screw pullout'. The following observations are worth noting on the morphology evolution displayed in Fig. 11. At the front end of the first kneading block (position A) where the barrel temperature was set at 160°C, we observe a poorly developed morphology which, again, is due to the rather low barrel temperature. However, at the exit of the first kneading block (position B) we clearly observe a dispersed morphology in which the PS droplets are dispersed in the HDPE matrix. The same dispersed morphology persists at position C where the barrel temperature was set at 200°C and at the second kneading block (position D). However, at position E where the barrel temperature was set at 210–220°C we observe a co-continuous morphology, and at the third kneading block (position F) where the barrel temperature was set at 230°C, we observe some breakdown of interconnected structures, and finally at position G, where the barrel temperature was set at 240°C, we observe a dispersed morphology in which the more viscous, minor component HDPE forms droplets and the less viscous, major component PS forms the continuous phase. We conclude that a phase inversion took place inside the extruder while the 70/30 PS/HDPE blend was melt blended.

Fig. 12 gives SEM images describing the morphology evolution in 50/50 PS/HDPE blend along the extruder axis, and a schematic describing barrel temperature profile and positions where blend specimens were taken after 'screw pullout'. The following observations are worth noting on the morphology evolution displayed in Fig. 12. At the first kneading block (position A) where the barrel temperature was set at 160°C, we observe a dispersed morphology in which the discrete phase of PS having irregular shapes is dispersed in the continuous phase of

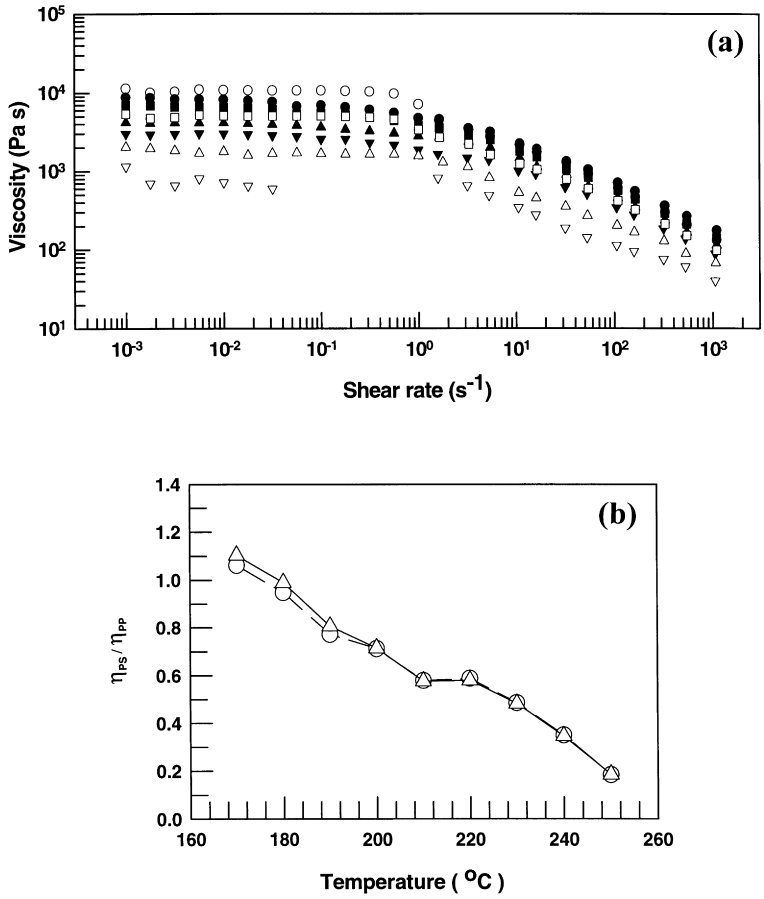

Fig. 14. The upper panel describes the shear rate dependence of viscosity for PS (open symbols) and PP (filled symbols) at various temperatures: (○, ●) 190°C; (□, ■) 200°C; (△, ▲) 220°C; (▽, ▼) 240°C. The lower panel describes the temperature dependence of viscosity ratio, η_{PS}/η_{PP}, at $\dot{\gamma} = 1500\ s^{-1}$ (○) and at $\dot{\gamma} = 500\ s^{-1}$ (△).

HDPE. Owing to the low barrel temperature at 160°C which is slightly above the T_{cf} ($\approx$ 155°C) of PS, the state of dispersion is rather poor. Interestingly enough, however, at position C where the barrel temperature was set at 200°C we observe a co-continuous morphology with interconnected structures of PS and HDPE. At the second and third kneading blocks (positions E and F) we still observe a co-continuous morphology. The same morphology persists along the rest of the extruder axis. However, in the extrudate (position H) we observe a dispersed morphology in which the HDPE forms droplets dispersed in the PS matrix. It is of great interest to observe in Fig. 12 that a phase inversion took place from one mode of dispersed morphology to another mode inside the extruder, while the 50/50 PS/HDPE blend was extruded.

Fig. 13 gives SEM images describing the morphology evolution in the 30/70 PS/HDPE blend along the extruder axis, and a schematic describing barrel temperature profile and positions where blend specimens were taken after 'screw pullout'. The following observations are worth noting on the morphology evolution displayed in Fig. 13. At the first kneading block (positions A and B) where the barrel temperature was set at 160°C we observe a dispersed morphology in which PS domains are dispersed in the HDPE matrix. It should be remembered that the T_{cf} of PS is 155°C and the T_m of HDPE is 125°C (see Table 2), and that at 160°C the viscosity of HDPE is lower than that of PS (see Fig. 10). Therefore, before reaching the T_{cf} of PS, the HDPE already melted and formed the continuous phase. At position C where the barrel temperature was set at 200°C we observe a slightly improved blend morphology, and in the second kneading block (position D) we clearly observe a much improved dispersed morphology in which PS droplets are dispersed in the HDPE matrix. Along the remainder of the extruder axis, we observe little change in blend morphology. Based on the above observations we conclude that in the 30/70 PS/HDPE blend, blend ratio determined the state of dispersion. This observation is consistent with that made above for the 30/70 PMMA/PS and 30/70 PC/PS blends.

3.2.2. PS/PP blends

Fig. 14(a) describes the dependence of viscosity of PS and PP, respectively, on shear rate ($\dot{\gamma}$) at various temperatures ranging from 190 to 240°C, and Fig. 14(b) describes the dependence of viscosity ratio, η_{PS}/η_{PP}, on temperature

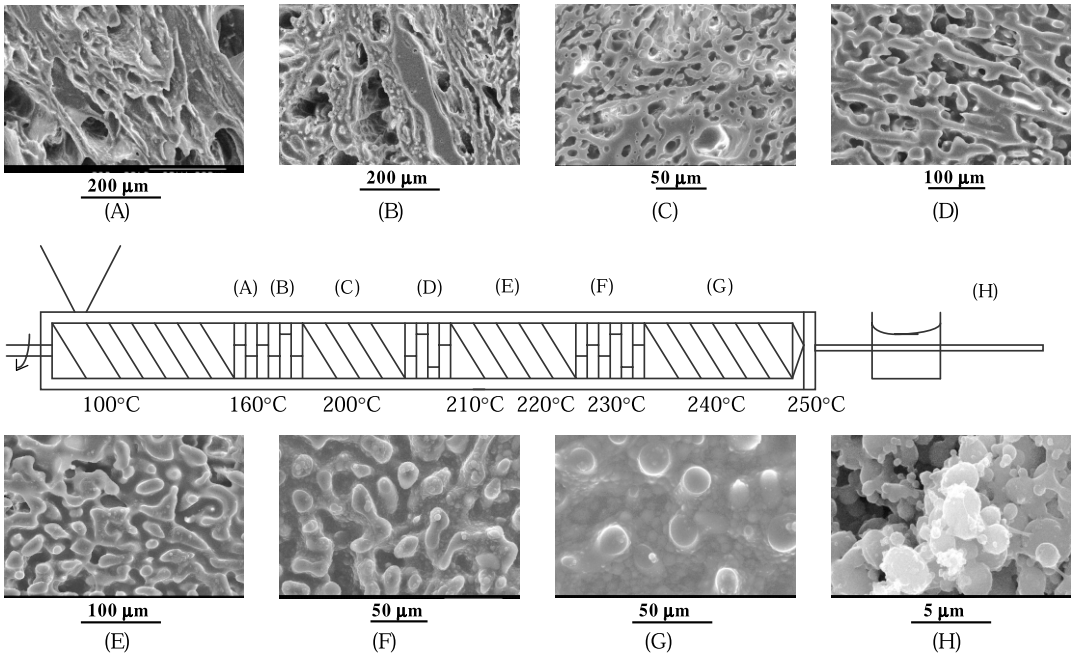

Fig. 15. The evolution of morphology in 70/30 PS/PP blend during compounding in a twin-screw extruder: (A) at the front end of the first kneading block (160°C); (B) at the exit of the first kneading block (160°C); (C) between the first and second kneading blocks (200°C); (D) at the front end of the second kneading block (210°C); (E) between the second and third kneading blocks (220°C); (F) at the exit of the third kneading block (230°C); (G) between the third kneading block and the die (240°C); (H) extrudate.

at $\dot{\gamma} = 1500$ and $500\ s^{-1}$, respectively, showing that η_{PS}/η_{PP} decreases with increasing temperature. It can be seen in Fig. 14 that (i) at 190°C the viscosity of PS is higher than that of PP at low shear rates, but the viscosities of the two polymers cross each other at higher shear rates, and (ii) at higher temperatures (200–240°C) the viscosity of PP becomes higher than that of PS.

Fig. 15 gives SEM images describing the morphology

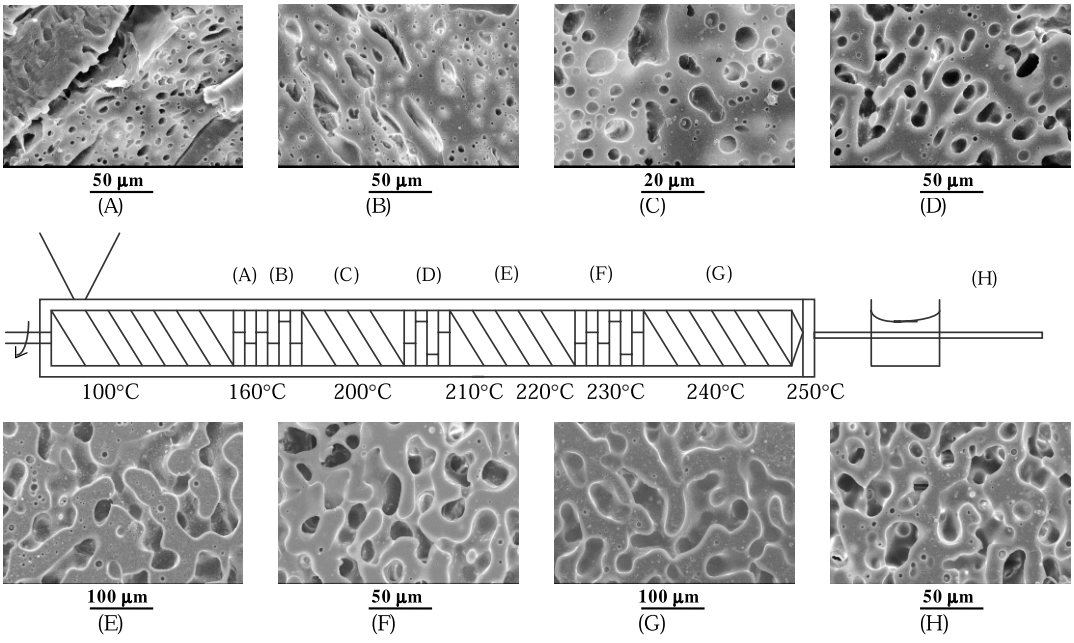

Fig. 16. The evolution of morphology in 50/50 PS/PP blend during compounding in a twin-screw extruder: (A) at the front end of the first kneading block (160°C); (B) at the exit of the first kneading block (160°C); (C) between the first and second kneading blocks (200°C); (D) at the front end of the second kneading block (210°C); (E) between the second and third kneading blocks (220°C); (F) at the exit of the third kneading block (230°C); (G) between the third kneading block and the die (240°C); (H) extrudate.

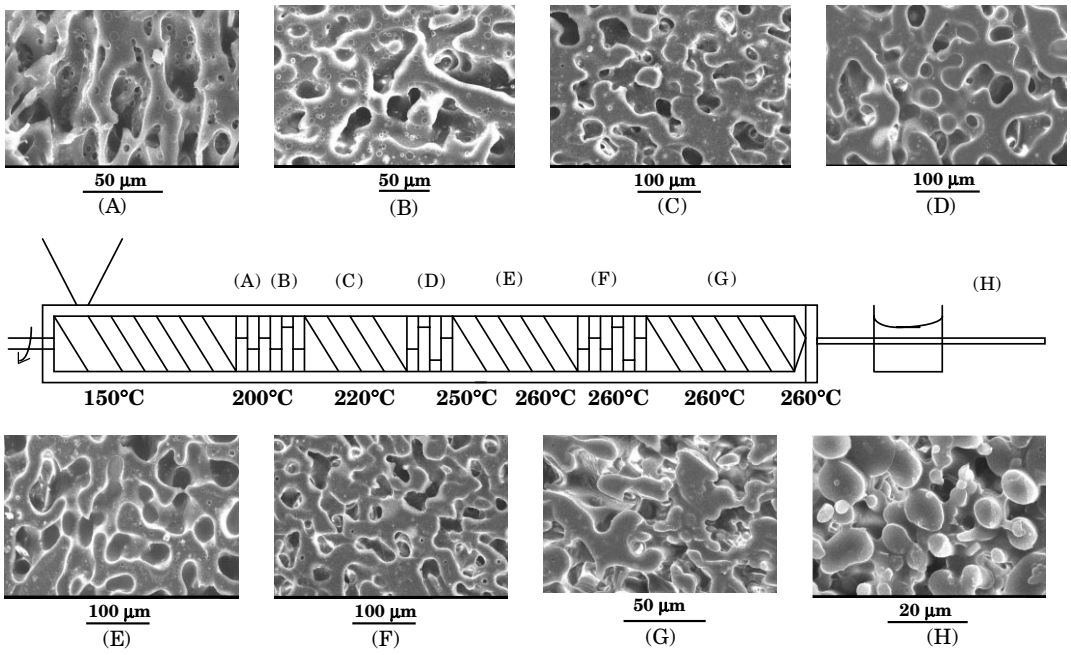

Fig. 17. The evolution of morphology in 50/50 PS/PP blend during compounding in a twin-screw extruder: (A) at the front end of the first kneading block (200°C); (B) at the exit of the first kneading block (200°C); (C) between the first and second kneading blocks (220°C); (D) at the front end of the second kneading block (250°C); (E) between the second and third kneading blocks (260°C); (F) at the exit of the third kneading block (260°C); (G) between the third kneading block and the die (260°C); (H) extrudate.

evolution in 70/30 PS/PP blend along the extruder axis, and a schematic describing barrel temperature profile and positions where blend specimens were taken after 'screw pull-out'. The following observations are worth noting on the morphology evolution displayed in Fig. 15. In the first kneading block (positions A and B),where the barrel temperature was set at 160°C, we observe many interconnected thin stands of PP dispersed in the PS matrix. At position C where

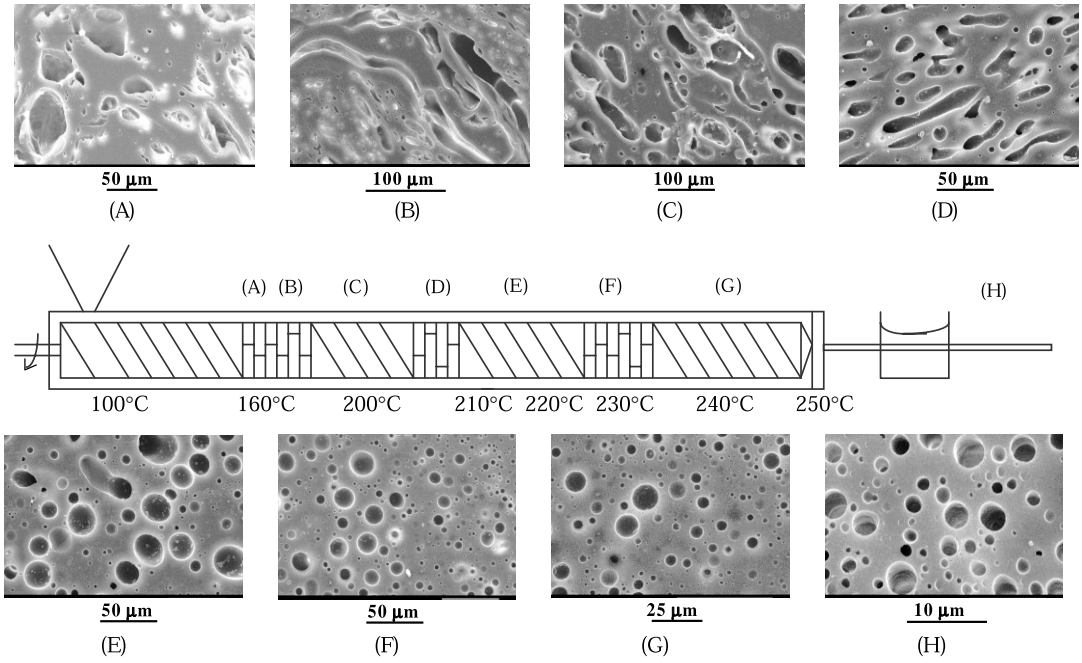

Fig. 18. The evolution of morphology in 30/70 PS/PP blend during compounding in a twin-screw extruder: (A) at the front end of the first kneading block (160°C); (B) at the exit of the first kneading block (160°C); (C) between the first and second kneading blocks (200°C); (D) at the front end of the second kneading block (210°C); (E) between the second and third kneading blocks (220°C); (F) at the exit of the third kneading block (230°C); (G) between the third kneading block and the die (240°C); (H) extrudate.

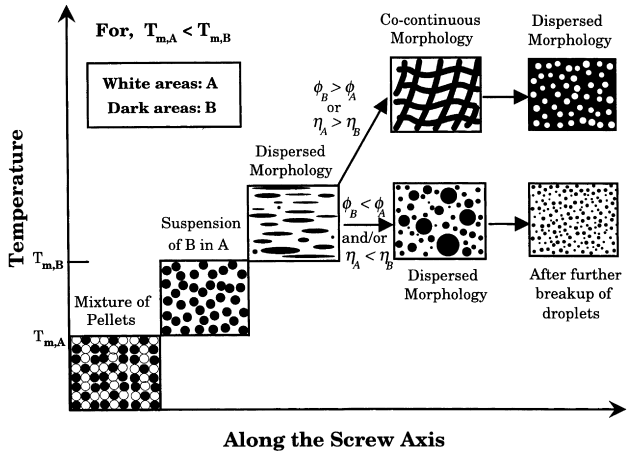

Fig. 19. Schematic diagram describing the evolution of blend morphology of a pair of immiscible polymers, A and B, along the axis of a twin-screw extruder, where the melting point of polymer A is assumed to be lower than that of polymer B.

the barrel temperature was set at 200°C we observe a mixture of a co-continuous morphology and a dispersed morphology. However, in the second kneading block (position D) we clearly observe a co-continuous morphology. At position E where the barrel temperature was set at 210–220°C we observe a breakdown of interconnected structures of PP, yielding broken droplets of irregular shape dispersed in the PS matrix. Interestingly, in the third kneading block (position F) where the barrel temperature was set at 230°C we observe elongated PP droplets dispersed in the PS matrix, and the droplets become spherical at position G where the barrel temperature was set at 240°C. The extrudate (position H) has a dispersed morphology in which PP droplets are dispersed in the PS matrix. Again, we observe that the more viscous, minor component PP forms droplets and the less viscous, major component PS forms the continuous phase.

Fig. 16 gives SEM images describing the morphology evolution in 50/50 PS/PP blend along the extruder axis, and a schematic describing barrel temperature profile and positions where blend specimens were taken after 'screw pullout'. The following observations are worth noting on the morphology evolution displayed in Fig. 16. At the front end of the first kneading block (position A) where the barrel temperature was set at 160°C, we observe a very poorly developed blend morphology, which is attributed to the low barrel temperature. However, at the exit of the first kneading block (position B) we observe a dispersed morphology in which the discrete phase of PS is dispersed in the PP matrix. We observe a dispersed morphology at position C, where the barrel temperature was set at 200°C, and at the second kneading block (position D). At position E where the barrel temperature was set at 210–220°C, we begin to observe a co-continuous morphology with interconnected structures of PS and PP. The same morphology persists along the rest of the extruder axis. However, as can be seen in Fig. 17, when the barrel temperature was increased to 220°C at position C, to 250–260°C at position E, and to 260°C at positions F and G before the 50/50 PS/PP blend leaves the extruder, we observe a transformation taking place from a co-continuous morphology to a dispersed morphology, in which the more viscous component PP forms the discrete phase dispersed in the less viscous PS (see Fig. 14(b) for the η_{PS}/η_{PP} ratio as a function of temperature). The above observation leads us to conclude that for the symmetric blend ratio the viscosity ratio plays the predominant role in determining the mode of dispersion, consistent with observations made above for the PMMA/PS, PC/PS, and PS/HDPE blends. Comparison of Fig. 16 with Fig. 17 demonstrates clearly that under the right processing conditions, a co-continuous morphology can be transformed into a dispersed morphology, confirming our previous observation that a co-continuous morphology is not a stable morphology [15].

Fig. 18 gives SEM images describing the morphology evolution in 30/70 PS/PP blend along the extruder axis, and a schematic describing barrel temperature profile and positions where blend specimens were taken after 'screw pullout'. The following observations are worth noting on the morphology evolution displayed in Fig. 18. In the first kneading block (positions A and B) where the barrel temperature was set at 160°C we observe a dispersed morphology, though not well developed, in which PS domains are dispersed in the PP matrix. We believe that owing to viscous shear heating, although the T_m of PP is 165°C the melting of PP occurred at least partially inside the first kneading block. At position C where the barrel temperature was set at 200°C we observe slightly improved blend morphology, and at position E where the barrel temperature was set at 210–220°C we clearly observe a much improved dispersed morphology. Along the remainder of the extruder axis, we observe little change in blend morphology. Based on the above observations we conclude that in the 30/70 PS/PP blend, blend ratio determined the state of dispersion. This observation is consistent with that made above for the 30/70 PMMA/PS, 30/70 PC/PS, and 30/70 PS/HDPE blends.

4. Discussion

We have shown that the morphology of binary blends of immiscible polymers, during melt blending in a twin-screw extruder, depends, among many factors, on (i) the melt blending temperature relative to the melting temperature (T_m) of a crystalline polymer and the critical flow temperature (T_{cf}) of an amorphous polymer, (ii) the screw speed (the intensity of mixing), (iii) duration of mixing (thus the residence time), (iv) the viscosity ratio of the constituent components, and (v) the blend composition.

The experimental observations made in this study can be summarized as schematically shown in Fig. 19, where we

assume that two *crystalline* polymers are melt blended in a twin-screw extruder. The same observations can be made when two *amorphous* polymers are melt blended in a twin-screw extruder, by simply replacing T_m appearing in Fig. 19 with T_{cf}. For illustration, let us consider that a PMMA/PS blend is melt blended in a twin-screw extruder. According to Fig. 19, we expect that PS, which has T_{cf} lower than that of PMMA, will first form a continuous phase in which solid (or rubber-like solid) PMMA particles will be suspended until the mixture travels down the extruder where the barrel temperature is higher than the T_{cf} of PMMA. Beyond that position, the evolution of blend morphology would depend on blend composition or viscosity ratio of PMMA and PS. Specifically, when the PMMA in a PMMA/PS blend is the *minor* component and *more viscous*, the PMMA will form the discrete phase and the PS will form the continuous phase. On the other hand, when the PMMA in a PMMA/PS blend is the *major* component and *more viscous*, the PMMA will form the continuous phase and the PS will form the discrete phase. Indeed we found that the above observations hold for all four blend systems investigated in this study. That is, we found that blend ratio determined the morphology of *asymmetric* blend compositions, and viscosity ratio determined the morphology of *symmetric* or *nearly symmetric* blend compositions.

However, from the point of view of the minimum energy dissipation principle in channel flow of two immiscible liquids, the component having lower viscosity is expected to form the continuous phase, wetting the channel wall where the shear stress is the greatest. In this regard, in the 70/30 PMMA/PS blend investigated in this study, for example, we expect that the more viscous PMMA would form the discrete phase and the less viscous PS would form the continuous phase. But our experimental results show the opposite in that, the PMMA formed the continuous phase and the PS formed the discrete phase. The same observation was found to hold for the other three blend systems investigated. The above observation suggests that a very delicate relationship, which controls the state of dispersion in an immiscible polymer blend, exists between blend ratio and viscosity ratio. In our previous paper [15] which dealt with the evolution of blend morphology during compounding in an internal mixer (Brabender Plasticorder), we made the same observations as described above. It should be mentioned that in the use of a Brabender mixer, we varied the mixing time up to 30 min, which was sufficiently long, ensuring that the observed morphology evolution was little to do with kinetic limitations.

Earlier, Jordhamo et al., [21] obtained an empirical relationship predicting phase inversion in a polymer blend in terms of the viscosity ratio (η_1/η_2) and blend ratio (ϕ_2/ϕ_1); namely, (i) when $(\eta_1/\eta_2)(\phi_2/\phi_1) > 1$, component 1 forms the discrete phase and component 2 forms the continuous phase; (ii) when $(\eta_1/\eta_2)(\phi_2/\phi_1) < 1$, component 2 forms the discrete phase and component 1 forms the continuous phase, and (iii) when $(\eta_1/\eta_2)(\phi_2/\phi_1) \approx 1$, a co-continuous morphology is expected. Here η_1 and η_2 are the viscosities of components 1 and 2, respectively, and ϕ_1 and ϕ_2 are the volume fractions of components 1 and 2, respectively. It should be mentioned that this relationship was obtained from limited experiments performed on binary blends of polystyrene and polybutadiene at very low shear rates (i.e. in the Newtonian regime) and thus it is *not* applicable to a pair of immiscible polymers exhibiting shear-thinning (i.e. non-Newtonian) behavior. We found that our experimental results deviate from such an empirical relationship.

Very recently, by formulating a system of equations for calculating the rate of energy dissipated per unit volume of fluid Han et al. [22] presented a theory predicting the mode of dispersion in two-phase flow in terms of the viscosity ratio and blend ratio of the constituent components. In doing so, they considered two modes of dispersed morphology: (i) Morphology I having a droplet of liquid A dispersed in the matrix phase of liquid B and (ii) Morphology II having a droplet of liquid B dispersed in the matrix phase of liquid A. They solved via a finite element method the system equations when a unit cell, having either Morphology I or Morphology II, was subjected to steady-state simple shear flow by using a criterion that the morphology that requires a lower rate of energy dissipated per unit volume in dispersed two-phase flow is a stable blend morphology. We have found that the theoretical predictions of blend morphology from the analysis of Han et al. [22] cannot explain some experimental results reported in this study.

5. Concluding remarks

There are two important conclusions that can be drawn from this study. They are: (i) the T_{cf} of an amorphous polymer plays an important role in determining the *initial* morphology during compounding of two immiscible polymers (at least one of which is amorphous) in a twin-screw extruder, and (ii) the instability of a co-continuous morphology.

We have demonstrated that the conventional view that the T_g of an amorphous polymer may be regarded as being equivalent to the softening temperature *cannot* explain the morphology evolution in a binary polymer blend at or near the first kneading block of a twin-screw extruder, where the softening and/or melting of polymers take place. However, using the concept of 'critical flow temperature' [16], we were able to explain the *initial* blend morphology in PMMA/PS, PC/PS, PS/HDPE, and PS/PP blends.

We have also demonstrated that a co-continuous morphology may be formed, irrespective of blend composition, when the extruder barrel temperature at or near the first kneading block, where the melting or softening of a polymer takes place, is lower than or slightly above the T_{cf} of an amorphous polymer, and that a co-continuous morphology can be made to transform into a dispersed morphology by raising the barrel temperature much higher than T_{cf}. On the

basis of the experimental observations made in this study, we conclude that a co-continuous blend morphology, observed under certain processing conditions in this study, is *not* stable and it is rather a transitory morphology that appears when one mode of dispersed morphology (where droplets of component A are dispersed in the matrix phase of B) transforms into another mode (where droplets of component B are dispersed in the matrix phase of A), i.e. when a phase inversion takes place during compounding.

We are well aware of the fact that different screw geometries might have produced different domain sizes in a dispersed morphology. In view of the fact that there can be many variations of screw geometry, and further, at present there is no theoretical guideline as to how different screw geometries might produce different domain sizes, in this study we did not vary screw configurations. Hence, we did not make an attempt to relate the sizes of dispersed domains to processing conditions. We believe that the mechanism of morphology development in immiscible polymer blends uncovered in this study will be valid regardless of screw configurations. In other words, the underlying principles that determine morphology evolution in polymer blends are believed to be independent of screw configurations. This speculation is yet to be confirmed by further experimental investigation in the future.

In the past some research groups [23–25] made attempts to model the flow of two immiscible polymers in a twin-screw extruder by considering it as a single-phase flow. Specifically, prediction of the pressure profile of two immiscible polymers along the axis of a twin-screw extruder is *not* meaningful without considering the two-phase nature of the flow, i.e. without considering morphology evolution in the twin-screw extruder, because the bulk viscosity of the blend depends, among many factors, on blend morphology. Thus, such attempts should *not* be regarded as being rigorous, because the flow of two immiscible polymers forming either a co-continuous or dispersed morphology during compounding in a twin-screw extruder, as shown in this paper, *cannot* be regarded as being equal to the flow of a homogeneous polymer. That is to say, any theoretical attempt to describe the flow of two immiscible polymers in a twin-screw extruder must include morphology evolution during compounding, suggesting that the mixing of two immiscible polymers with proper moving boundary conditions at the phase interface be included. As presented in this paper, in addition to the deformation of droplets, breakup and coalescence of droplets also would occur during compounding under certain processing conditions. However, the consideration of the breakup and coalescence of droplets during compounding of two immiscible polymers in a twin-screw extruder is meaningful *only when* one first has information on the mode of dispersion, i.e. which (A or B) of the two polymers forms droplets and dispersed in the other polymer. To the best of our knowledge, theoretical treatment of morphology evolution during compounding of two immiscible polymers in a twin-screw extruder has not been addressed in the literature. Any serious attempt in the future to model the flow of two immiscible polymers in a twin-screw extruder must include the evolution of two-phase morphology, including breakup and coalescence of droplets, along the extruder axis. No doubt that this is a very complex and difficult subject that requires greater attention in the future.

References

[1] Han CD, Yu TC. Polym Eng Sci 1972;12:81.
[2] Han CD, Kim YW. Trans Soc Rheol 1975;19:245.
[3] Han CD. Rheology in polymer processing. New York: Academic Press, 1976. Chapter 7.
[4] Han CD. Multiphase flow in polymer processing. New York: Academic Press, 1981. Chapter 4.
[5] Nelson CJ, Avgeropoulos GN, Weisser FC, Böhm GGA. Angew Makromol Chem 1977;60/61:49.
[6] Van Oene H. In: Paul DR, Newman S, editors. Polymer blends, vol. 1. New York: Academic Press, 1978. p. 295–352.
[7] Miles IS, Zurek A. Polym Eng Sci 1988;28:796.
[8] Ho RM, Wu CH, Su AC. Polym Eng Sci 1990;30:511.
[9] Favis BD, Therrien D. Polymer 1991;32:1474.
[10] He J, Bu W, Zeng J. Polymer 1997;38:6347.
[11] Shih C-K. Polym Eng Sci 1995;35:1688.
[12] Sundararaj U, Macosko CW, Shih C-K. Polym Eng Sci 1996;36:1769.
[13] Sundararaj U, Macosko CW, Rolando RJ, Chan HT. Polym Eng Sci 1992;32:1814.
[14] Scott CE, Macosko CW. Polymer 1995;36:461.
[15] Lee JK, Han CD. Polymer 1999;40:6277.
[16] Han CD, Lee KY, Wheeler NC. Polym Eng Sci 1996;36:1360.
[17] Karam H, Bellinger JC. Ind Eng Chem Fundam 1968;7:576.
[18] Torza S, Cox RC, Mason SGJ. Colloid Interface Sci 1972;38:395.
[19] Grace H. Chem Eng Commun 1982;14:225.
[20] Chin HB, Han CD. J Rheol 1980;24:1.
[21] Jordhamo G, Manson J, Sperling L. Polym Eng Sci 1986;26:517.
[22] Han CD, Sun J, Chuang KH, Lee JK. Polym Eng Sci 1998;38:1154.
[23] Meijer HEH, Elemans PHM. Polym Eng Sci 1988;28:275.
[24] Shi ZH, Utracki LA. Polym Eng Sci 1993;32:1834.
[25] Huneault MA, Shi ZH, Utracki LA. Polym Eng Sci 1995;35:115.